

# An extension of Newton’s apsidal precession theorem

S. R. Valluri,<sup>★1,2</sup> P. Yu,<sup>2</sup> G. E. Smith<sup>3</sup> and P. A. Wiegert<sup>1</sup>

<sup>1</sup>*Department of Physics and Astronomy, The University of Western Ontario, London, Ontario, Canada N6A 3K7*

<sup>2</sup>*Department of Applied Mathematics, The University of Western Ontario, London, Ontario, Canada N6A 3K7*

<sup>3</sup>*Department of Philosophy, Tufts University, Medford, MA, 02155-7059, USA*

Accepted 2005 January 5. Received 2004 September 29

## ABSTRACT

Newton’s apsidal precession theorem in Proposition 45 of Book I of the ‘Principia’ has great mathematical, physical, astronomical and historical interest. The lunar theory and the precession of the perihelion of the planet Mercury are but two examples of the applications of this theorem. We have examined the precession of orbits under varying force laws as measured by the apsidal angle  $\theta(N, e)$ , where  $N$  is the index for the centripetal force law, for varying eccentricity  $e$ . The paper derives a general function for the apsidal angle, dependent only on  $e$  and  $N$  as the potential is spherically symmetric. Further, we explore approximate ways of the solution of this equation, in the neighbourhood of  $N = 2$  which happens to be the case of greatest historical interest. Exact solutions are derived where they are possible. The first derivatives  $\partial\theta/\partial N$  and  $\partial\theta/\partial h$  [where  $h(N, e)$  is the angular momentum] are analytically expressed in the neighbourhood of  $N = 2$  (case of the inverse square law). The value of  $\partial\theta/\partial N$  is computed numerically as well for  $1 \leq N < 3$ . The resulting integrals are interesting improper integrals with singularities at both limits. Some of the integrals, especially for  $N = 2$ , can be given in closed form in terms of generalized hypergeometric functions which are reducible in terms of algebraic and logarithmic functions. No evidence was found for isolated cases of zero precession as  $e$  was increased. The  $N = 1$  case of the logarithmic potential is also briefly discussed in view of its interest for the dynamics of eccentric orbits and its relevance to realistic galaxy models. The possibility of apsidal precession was also examined for a few cases of high-eccentricity asteroids and extrasolar planets. We find that these systems may provide interesting new laboratories for studies of gravity.

**Key words:** gravitation – celestial mechanics – Solar system: general.

## 1 INTRODUCTION

In Proposition 45 of Book I of the ‘Principia’ (Newton 1687), Newton derives an important formula relating centripetal force, expressed as a power of the distance from the centre, to the apsidal angle,  $\theta$ , or angle at the force centre between highest and lowest apsis (apocentre and pericentre). For a centripetal force of magnitude  $\mu r^{n-3}$ ,  $\theta = \pi/\sqrt{n} = 180^\circ/\sqrt{n}$ . The formula, by its manner of derivation, is restricted to orbits ‘approaching very near to circles’ ( $e \ll 1$ ).

The apsides are termed ‘quiescent’ if  $n = 1$ , and ‘moving’ if  $n \neq 1$ . In the latter case the orbiting body in going from upper to lower apse moves through either more or less than  $180^\circ$ , and the same angle is repeated in the return to the upper apse. In this case we shall say that the orbit precesses. Given Newton’s formula, the amount of precession measures the exponent in the force law. Zero

precession (where  $n = 1$ ) is equivalent to having the force vary as the inverse square of the distance. Positive precession (prograde or advancing orbit where  $n < 1$ ) is equivalent to having the force fall off more rapidly with distance than does an inverse-square force; the exponent in the force law is less than  $-2$ . Negative precession (retrograde, where  $n > 1$ ) is equivalent to having the force fall off less rapidly with distance than does an inverse-square force; the exponent in the force law is greater than  $-2$ . Where Newton’s formula is applicable, an empirical determination of the amount of precession yields a measure of the exponent in the force law.

In Book III of the Principia, Newton cites Proposition 45 in arguing that the force of the Sun on the planets is inversely as the square of the distance (Proposition 2: the planetary aphelia are ‘quiescent’, whence the force is inverse square). At the time Newton had reason (from Streete’s ‘Astronomia Carolina’) to think that the orbits of the planets were not detectably precessing; during the course of the next century, as the time period over which reliable planetary observations had been made grew, it became clear that these orbits were slowly precessing. (Laplace chooses not to infer the inverse square

<sup>★</sup>E-mail: valluri@uwo.ca

for the planets from the precession theorem, probably because he could no longer run the simple argument Newton has run in Book 3, Proposition 2.) Again citing Proposition 45, Newton argues that the force of the Earth on the Moon varies in the inverse-square proportion (Proposition 3: the lunar apsis moves on average  $3\text{:}3$  arcmin per revolution, whence  $n - 3 = -2(4/243)$ , the small deviation from the inverse-square proportion being attributable – so Newton promises to show – to the radial component of the perturbing action of the Sun) (Newton 1687). For an orbit that is bounded away from infinity, we can define orbital eccentricity by  $e = (r_M - r_m)/(r_M + r_m)$ , where  $r_M$  is the greatest distance from the centre, and  $r_m$  the least. This definition reduces to the usual measure of eccentricity for an ellipse, and has the additional merit of being applicable to the planetary orbits, none of which is strictly an ellipse (the apsidal angle in all cases differs from  $180^\circ$ , Newton’s ‘quiescence of the apsides’ being only approximate). These orbits, though non-re-entrant, have a greatest and least distance from the centre of force, and hence have an eccentricity in the sense of our definition.

Newton apparently trusts his formula even where the eccentricity is not close to zero. In Proposition 2 of Book III, for instance, he in effect applies it to the orbit of Mercury, whose eccentricity is 0.2056, so that the greatest solar distance is 1.5 times the least. In the General Scholium where he speaks of the possibility of quiescent apelia for the orbits of comets, he no doubt has in mind Halley’s comet, which, as Halley proposed in 1705, has an orbital eccentricity of about 0.97, so that the greatest solar distance is 66 times the least; this is hardly, it would seem, the case for Proposition 45.

We investigated, in Valluri, Wilson & Harper (1997), for force laws other than the inverse square as well as differing but slightly from the inverse square, what happens to the apsidal angle as the orbital eccentricity increases. In this work, we discuss the apsidal angle and its derivative for a variety of force laws with different power index  $N$ . We also study the force law for the inverse power of the distance, i.e. the logarithmic potential. Such a force law has become increasingly relevant, owing to recent photometric observations of nearly elliptical galaxies and spiral galaxies, as pointed out by Touma & Tremaine (1997). Such studies are of relevance for orbital dynamics.

An interesting question that arose is the dependence of the apsidal angle  $\theta$  for cases where  $\delta = N - 2$  is either very small or less than one (Valluri et al. 1997). MATHEMATICA and MAPLE labour for hours at the integration for very small  $\delta$  to obtain  $\theta$  without providing numerical results. It is desirable then to examine the derivative  $\partial\theta/\partial N = \partial\theta/\partial\delta$  and also  $\partial\theta/\partial h$  (where  $h(N, e)$  is the angular momentum) to thereby obtain  $\theta$ . In the previous work (Valluri et al. 1997), the derivative was calculated numerically only for the case  $\delta \rightarrow 0$  and  $\theta(N, e)$  was numerically evaluated for  $N = 3/2, 7/4, 2, 9/4$  and  $5/2$ . A detailed analysis of the derivative in the interval  $1 \leq N < 3$  warrants a careful study. In addition, the analytical calculation of the apsidal angle and its derivative, when  $\delta$  is very small, offers additional insight. The differential equation of the orbit in this paper is studied from an approach similar to that of Clairaut in his study of the lunar orbit (Brown 1895). The resulting series solutions have intrinsic mathematical interest of their own. The expression for the angle  $\theta$  can be differentiated under the integral sign. The resulting improper integrals offer an important mathematical study. Moreover, they illustrate for each eccentricity  $e$  the dependence of  $\theta(N)$  and confirm the absence of isolated cases of apsidal quiescence. The lunar theory, the orbit of Mercury, gravitational waves emitted during the orbital decay of black hole (BH) binaries (Peters & Mathews 1963; Peters 1964; Pierro et al. 2002) as well as luminosity power-law densities near the centres of many nearly elliptical galaxies have rekindled

interest in Newton’s apsidal precession theorem. The researches of Euler, Lagrange, Laplace, Hill, Hansen, Tisserand, Hall, Newcomb, Poincaré (Brown 1895) and many others as well as the general theory of relativity of Einstein have given this problem of celestial mechanics a new stimulus.

The calculation of the partial derivative  $\partial\theta/\partial h$  has an interesting parallel to the partial derivatives of the potential scattering phase shift with respect to physical quantities such as linear and orbital angular momentum, and which has possible application in a variety of fields that range from electron scattering from ions, heavy-ion scattering in nuclear physics and resonance scattering to scalar waves scattering in a gravitational field by rotating BHs. Much of the physical information contained in the scattering phase shifts  $\delta(h, l)$  can be extracted from their partial derivatives with respect to such physical quantities as linear momentum (Romo & Valluri 1998) and angular momentum, associated with time delay and the deflection function (Valluri & Romo 1989, 1994) and other potential parameters. The deflection function  $2\partial\delta(l, k)/\partial l$  is of relevance for rainbow and glory scattering in semiclassical collisions in a variety of problems that include scattering in BH gravitational fields. The analytic method supported by numerical analysis is also relevant for calculations of the deflection function in Schwarzschild and Kerr geometries for rainbow and glory scattering. Kostas Glampedakis & Andersson (2001) have investigated the scattering of massless scalar waves by a Kerr BH. They show that although the pioneering work of Ford and Wheeler considered scattering in the context of quantum theory, their formalism is readily extended to the black-hole case. In the semiclassical paradigm, the phase-shifts are approximated by a one-turning point JWKB formula. Partial derivatives of the phase shift can also be obtained for long ranged potentials like the gravitational one, a repulsive exponential potential, Hulthen, Sech-square, Morse valley and barrier potentials. The Regge–Wheeler equation (Regge & Wheeler 1957), describing a scattering process in a BH space time, is similar to the radial Schrodinger equation and many techniques from quantum and classical scattering can be applied to BH problems. Both  $\partial\delta(l)/\partial l$  and  $\partial\delta(k)/\partial k$  are of relevance in BH scattering. The tortoise coordinate in the treatment of the Regge–Wheeler equation, is related to the Lambert W function discussed in the work of Valluri, Jeffrey & Corless (2000), and facilitates the treatment of wave scattering in curved space time. In particular, glory scattering and orbiting phenomena in the mathematical theory of BHs have been thoroughly discussed by Chandrasekhar (1983).

In the next section we discuss the case of force laws differing but slightly from the inverse square. The differential equation of the orbit is studied to obtain the equation of an ellipse with rotating apsis. The apsidal angle and its derivative with respect to  $N$  (or equivalently  $\delta$ ) are derived in terms of the eccentricity  $e$ .

In Section 3 we extend our results to the case of force laws differing considerably from the inverse square and calculate  $\partial\theta(e)/\partial N$  for such laws. Section 4 presents the conclusions and discussion.

## 2 THE CASE OF FORCE LAWS DIFFERING BUT SLIGHTLY FROM THE INVERSE SQUARE

That the force law differs but slightly from the inverse square was the hypothesis that Asaph Hall made in 1894, in seeking to account for the anomalous precession of the apse of Mercury (Hall 1894). In 1859 Le Verrier (Le Verrier 1859) had found that some 38 arcsec per century of the precession of the apse of Mercury could not be accounted for on the basis of Newton’s inverse-square law, and in 1882 Simon Newcomb revised this estimate upward to 43 arcsec per century (Newcomb 1882). Taking the gravitational law to be

given by  $-\mu r^{-N}$ , Hall used the formula  $\pi/\sqrt{3-N}$ , where  $3-N$  was  $n$  in Newton's notation, to deduce from 43 arcsec per century a law in which the exponent  $N = 2.00000016$ . Hall was apparently unaware of Newton's derivation of the formula  $180^\circ/\sqrt{n}$ ; he cited instead a paper by Joseph Bertrand from which the formula can be derived (Bertrand 1873). But Bertrand's argument, like Newton's, assumes that the greatest and least distances to the centre of force differ infinitesimally. Is the formula validly applicable to the orbit of Mercury? And more generally, does precession measure deviation from the inverse-square law even when the eccentricity is sizable?

To address this question, we turn to the differential equation of the orbit. Let the central force be given by  $f(r) = -\mu r^{-N}$ , where  $\mu$  is a constant (choose  $\mu = 1$ ). We assume  $N > 0$ , so that  $f(r) \rightarrow 0$  as  $r \rightarrow \infty$ . The standard differential equation for the shape of the orbit, expressed in terms of the reciprocal radius vector,  $u = 1/r$ , and the angle about the centre of force,  $\theta$ , is

$$\frac{d^2 u}{d\theta^2} + u = \frac{u^\delta}{h^2}, \quad (1)$$

where  $N - 2 = \delta$  (Valluri et al. 1997). Here  $h$  (angular momentum) is twice the rate of the description of area  $r^2 (d\theta/dt) = h$ . In the cases we want to examine,  $\delta$ , which can be positive or negative, will be small enough in absolute value so that we can ignore its square. (In Hall's case it was  $-0.00000016$ .) To obtain an approximate solution of equation (1) in this case, we suppose  $u = u_0 + \Delta y$ , where  $u_0$  is the solution when  $\Delta y = 0$ , namely  $u_0 = [1 + e \cos(\theta - \theta')]/h^2$ , and  $\Delta y$  is a perturbation introduced to take account of the difference when  $\delta$  differs from zero.

Substituting this expression for  $u$  into equation (1), we obtain

$$\frac{1}{h^2} + \frac{d^2(\Delta y)}{d\theta^2} + \Delta y = \frac{1}{h^2}(u_0 + \Delta y)^\delta = \frac{u_0^\delta}{h^2} + \frac{\delta(\Delta y)u_0^{\delta-1}}{h^2}. \quad (2)$$

In expanding  $u_0^\delta$  on the right, we observe that, while we suppose  $\delta$  to be small enough so that its square may be neglected, we are allowing the eccentricity  $e$  to have any value in the interval  $0 < e < 1$ ; we shall thus take into account higher powers of the eccentricity than the first. If we neglect a small constant  $1/h^2 - 1/h^{2\delta+2}$ , equation (2) can be put in the form

$$\begin{aligned} \frac{d^2(\Delta y)}{d\theta^2} + (\Delta y) \left(1 - \frac{\delta}{h^{2\delta}}\right) \\ = \frac{\delta}{h^{2\delta+2}} \sum_{i=1}^{\infty} (-1)^{i+1} \left(\frac{e^i}{i}\right) \cos^i(\theta - \theta') \\ - \frac{\delta(\Delta y)}{h^{2\delta}} \sum_{i=1}^{\infty} (-1)^i e^i \cos^i(\theta - \theta'). \end{aligned} \quad (3)$$

Here we have shifted the constant term  $\delta(\Delta y)/h^{2\delta}$  to the left-hand side. All terms with the coefficient  $\delta(\Delta y)/h^{2\delta}$  will prove to be of  $O(\delta^2)$ , once we have shown that  $\Delta y$  is of  $O(\delta)$ . We shall discuss the solution of equation (3) with the second term on the right deleted (McLachlan 1947). Inclusion of this second term results in the differential equation of Hill which can be solved approximately by the theory and application of Mathieu functions (McLachlan 1947; Valluri et al. 1999). The resulting differential equation is mathematically analogous to that of a harmonic oscillator with a restoring force  $(1 - \delta/h^{2\delta})\Delta y$  and oscillating driving forces proportional to  $(-1)^{i+1} e^i \cos^i(\theta - \theta')/i$ . This is equivalent to a driving force which depends on the eccentricity  $e$ , a resonant term that builds up the precession and small amplitude higher harmonic periodic perturbations. The resulting equation is linear with constant coefficients; its general solution is therefore the sum of the complementary function

and a particular integral. If we let  $1 - \delta/h^{2\delta} = \lambda^2$ , the complementary function = const.  $\cos \lambda(\theta - \theta')$ . After further simplification we obtain

$$u_0 + \Delta y = \frac{1}{h^2} [1 + e \cos \lambda(\theta - \theta')] + O(\delta). \quad (4)$$

The terms of  $O(\delta)$  on the right are small relative to those free of the factor  $\delta$ ; neglecting them, we have the equation of an ellipse with rotating apse, which we can write as

$$u = \frac{1}{h^2} [1 + e \cos \lambda(\theta - \theta')]. \quad (5)$$

The apsidal angle is given by  $(\theta - \theta') = \pi/\lambda$ . To a near approximation,  $\lambda = 1 - \delta/2h^{2\delta} = 1 - \delta/2$ , as  $h^{2\delta}$  is close to unity because of the smallness of  $\delta$ . This turns out to be the same result that Newton's formula gives:  $\pi/\sqrt{n} = \pi/\sqrt{3-N} = \pi/\sqrt{1-\delta} = \pi/(1-\delta/2)$ . For  $\delta = 0$  (inverse square case) the result is  $\pi$ , as it should be. Newton's formula, we recall, is valid only for very small eccentricity. What role does the eccentricity play in our solution?

Clairaut was probably the first to publish a method for the treatment of the lunar theory founded on the integration of differential equations (Brown 1895). In the spirit of Clairaut's approach in his lunar theory, we adopt a rotating ellipse as a starting point

$$u = \frac{1}{h^2} [1 + e \cos \lambda'(\theta - \theta')], \quad (6)$$

where  $\lambda'$  will differ from  $\lambda$  as previously defined in such a way as to take account of the effect of eccentricity on apsidal angle. We substitute equation (6) back into equation (1), and as before neglect the small constant  $1/h^2 - 1/h^{2\delta+2}$ , and all terms involving  $\delta$  raised to a higher power than the first. We find that

$$1 - \lambda'^2 = \frac{\delta}{h^{2\delta}} \sum_{i=0}^{\infty} (-1)^i \frac{e^i}{i+1} \cos^i \lambda'(\theta - \theta'). \quad (7)$$

We can get an average result for the right-hand side by integrating it over the apsidal angle, from 0 to  $\pi$ , then dividing by  $\pi$ .

$$\begin{aligned} 1 - \lambda'^2 &= \frac{\delta}{h^{2\delta}} \left(1 + \frac{e^2}{6} + \frac{3e^4}{40} + \frac{5e^6}{112} + \dots\right) \\ &= \frac{\delta}{h^{2\delta}} \frac{\arcsin e}{e}. \end{aligned} \quad (8)$$

Further, in the course of our investigation, it was brought to our attention (Nauenberg, private communication) that  $\lambda'^2$  is given to third order in  $e_1$  by the formula

$$\lambda'^2 = (3-N) \left[1 - \frac{(N-2)(N+2)}{12} e_1^2\right], \quad (9)$$

where  $e_1$  is the first coefficient in the expansion  $u = u_0[1 + \sum_{n=1}^{\infty} e_n \cos(n\lambda'\phi)]$ ,  $e_2 = (1/12)(N-2)e_1^2$ ,  $e_3 = (1/96)(N-2)(N-3)e_1^3$ , and the eccentricity  $e$  is approximated by  $e \approx e_1 - e_2 + e_3$ . Equation (9) gives results for the apsidal angle,

$$\theta = \frac{\pi}{\lambda'} = \frac{\pi}{\left\{(3-N) \left[1 - (N-2)(N+2)e_1^2/12\right]\right\}^{1/2}}.$$

This formula gives results for the apsidal angle closely agreeing with those obtained by numerical integration (see Section 3). In addition, it implies that for  $N = 2.00000016$  as proposed by Asaph Hall, the square bracket is effectively 1, and  $\lambda$  is given with good accuracy by  $(3-N)^{1/2}$  in agreement with Newton's and Bertrand's formulas.

By this calculation, for  $\delta$  small enough so that  $h^{2\delta}$  can be taken as unity,

$$\lambda' = 1 - \frac{\delta}{2} \frac{\arcsin e}{e}, \quad (10)$$

and the apsidal angle  $\pi/\lambda'$  is approximately  $\pi(1 + \delta \arcsin e/2e)$ . Here  $\arcsin e/e > 1$ , and increases with increasing eccentricity. The lowest power of  $e$  entering into the formula is  $e^2$ , which implies that Newton's formula is accurate to first order in  $e$ . As we shall show later, equation (8) is qualitatively correct in that  $\delta/h^{2\delta}$  is multiplied by a factor that increases with increasing  $e$ ; however, the values it gives for the apsidal angles are a bit shy of the true values, the error increasing with increasing  $e$ . The derivative of the apsidal angle  $\theta$  with respect to the power-law index  $N$  or in terms of  $\delta$ , from the Clairaut type of approach, the perturbative analysis (Valluri et al. 1997) and Newton's formula are given below.

$$\frac{\partial\theta}{\partial\delta} \sim \frac{\pi}{2} \frac{\arcsin e}{e} \sim \frac{\pi}{2} \left( 1 + \frac{e^2}{6} + \frac{3e^4}{40} + \dots \right), \quad (11)$$

$$\frac{\partial\theta}{\partial\delta} \sim \frac{\pi}{2} \left( 1 + \frac{e^2}{4} + \frac{e^4}{8} + \dots \right), \quad (12)$$

$$\frac{\partial\theta}{\partial\delta} \sim \frac{\pi}{2} \frac{1}{(1-\delta)^{3/2}}. \quad (13)$$

Equation (13) is independent of  $e$  and gives accurate results only for almost vanishing  $e$ . For given  $\delta$ , precession, or the departure of the apsidal angle from  $180^\circ$ , becomes greater as the eccentricity increases. It follows that departure of the apsidal angle from  $180^\circ$  becomes a more sensitive index of departure from the inverse-square law as the eccentricity increases.

In the case of Mercury, with  $e = 0.2056$ , the fraction  $\arcsin e/e$  is 1.0072. Multiplying by  $\delta/2$  and by  $180 \times 3600$ , we find the extra precession per half cycle, namely 0.052 arcsec. Multiplying this result by 830.39, the number of half-cycles per Julian century, we obtain 43.20 arcsec, the extra precession per Julian century. Without the factor 1.0072, the result would be 43.05 arcsec, a difference of 0.3 per cent, rather less than the uncertainty in the empirical value of the precession. [In 1947 G.M. Clemence (Clemence 1947), taking into account all the observations of Mercury from 1765 to 1940, found the extra precession to be  $43.11 \pm 0.45$  arcsec per century.] For our Moon ( $e = 0.05493$ ) the derivative for equation (11) is  $(\pi/2)(1.000504)$ , for equation (12)  $(\pi/2)(1.000756)$  and for equation (13)  $\pi/2$ .

By 1903 Hall's alternative power law to account for the 43 arcsec of anomalous precession in the apsis of Mercury had become untenable: Ernest W. Brown's development of the Hill–Brown lunar theory was sufficiently detailed to rule out Hall's alternative power law (Brown 1903). In 1915 Einstein showed that the anomalous apsidal precession could be derived from his Theory of General Relativity (GR: Einstein 1915; Roseveare 1982; Earman & Janssen 1993).

Early discussions of alternative gravitational force laws took place largely within the context of the precession of the perihelion of Mercury. This small planet being closest to the Sun and on a relatively eccentric orbit suffers the largest GR-induced precession of any of the planets in our Solar system. Precession owing to differing force laws, however, is not confined to the region close to the Sun. Equation (10) is independent of the size of an orbit, but depends rather on its eccentricity. Both the precession rate of an orbit and the ease with which such precession is observed increase as the eccentricity of the orbit increases. As a result, observational limits of  $\delta$  can most easily be constructed by observing high-eccentricity objects. As the number of bodies known to be on high-eccentricity orbits has increased dramatically since early discussions of the effects, the number of opportunities for testing  $\delta$  directly in systems with different properties, such as high  $e$  and larger mass, has also grown.

The longest known and hence best observed objects on high- $e$  orbits are comets. However, these bodies suffer non-gravitational accelerations (i.e. accelerations owing to the back reaction of gases sublimating from the comet nucleus) that are difficult to quantify. For example, during its 1986 appearance, Comet Halley is thought to have experienced such back reaction forces of magnitude roughly  $10^{-5}$  of the gravitational force owing to the Sun (Rickman 1986). Additionally, the magnitude of this force varies with the distance of the comet from the Sun and its instantaneous direction is unknown, its determination complicated by such effects as variations between the pre- and post-perihelion legs of its orbit (Sekanina 1964; Festou 1986), variations in the outgassing on time-scales of order of a day (Festou, Rickman & West 1993) and rotation of the (potentially precessing) nucleus itself (Wilhelm 1987). Thus comets are not ideal candidates for measurements of  $\delta$ .

Asteroids are different from comet nuclei in being devoid of the volatile materials whose outgassing complicates the precise determination of the motion of a comet. Some extinct comets may lurk among the asteroid population and low-level outgassing may affect their motion, but the effect would be greatly reduced and the number of such objects is likely quite small (Levison et al. 2002). Though asteroids are typically on low-eccentricity orbits the population known to be on orbits of higher  $e$  has increased markedly over the past decades. For example, at this writing the Minor Planet Center lists 151 objects with  $e > 0.75$ , and 10 with  $e > 0.9$  (see Table 1). All of these have been discovered in the last 5 yr, with the exception of 5025 P-L and 1984 QY1, discovered in 1960 and 1984, respectively. Both were only observed for a few (3–4) days and are now considered lost. 2000 LK was only observed for 7 d, but 1999 XS35, 2000 SG8, 2001 DQ8, 2002 PD43, 2003 MT9 and 2004 CK39 have arc lengths from two to several weeks. The longest observational arc, and hence one of the better candidates for such measurements is 2002 AJ129, which has been observed for over a year. Its aphelion distance is far from Jupiter, reducing the effects of perturbations from this planet, and it will make a number of close approaches to within 0.1 au of Earth (in 2010, 2018 and 2026)

**Table 1.** High-eccentricity asteroids, their semimajor axis  $a$ , their inclination  $i$  along with their perihelion  $q$  and aphelion  $Q$  distances.

Name	1984 QY1	1999 XS35	2000 LK	2000 SG8	2001 DQ8	2002 AJ129	2002 PD43	2003 MT9	2004 CK39	5025 P-L
$e$	0.914	0.947	0.947	0.901	0.902	0.915	0.956	0.920	0.925	0.901
$a$ (au)	2.97	17.9	2.27	2.45	1.84	1.37	2.51	2.52	4.26	4.22
$i$ (deg)	17.8	19.4	17.4	24.0	13.0	15.5	26.3	6.81	14.7	7.34
$q$ (au)	0.255	0.954	0.119	0.242	0.181	0.117	0.111	0.202	0.320	0.417
$Q$ (au)	5.69	34.9	4.41	4.66	3.51	2.63	4.92	4.84	8.20	8.01

which should allow its orbit to be very accurately determined by radar.

We note that variations in the orbit of asteroid 6489 Golevka attributed to the Yarkovsky effect have recently been detected by radar (Chesley et al. 2003). The observation of this small effect, amounting to only 15 km in the range to the body, indicates that the measurement of other small perturbations may be possible. The eccentricity of the orbit of 6489 Golevka is substantial (0.6) and it may also provide a useful limit on the value of  $\delta$ , though the data published do not allow such a calculation.

Anomalous precession may also be observed outside our Solar system. The inspiralling orbits of stars into massive BHs, for example, are expected to display dramatic relativistic perihelion precession as they undergo orbital changes owing to the dissipation of energy and angular momentum as gravitational waves (cf. Barack & Cutler 2004). Planets orbiting other stars offer another opportunity. At the time of writing, there are 120 extrasolar planets known to be orbiting 105 stars. If in fact there is only one planet orbiting most of these stars as these numbers naively imply, then the determination of  $\delta$  becomes significantly easier as perturbations owing to other bodies do not need to be modelled. If, as is more likely the case, there are in fact other smaller planets present, the fact that the body being observed is likely the most massive in the system provides us with a significant advantage over our own Solar system where the largest bodies are on low-eccentricity orbits. Any perturbations such a planet suffers owing to other bodies in the system will be reduced in proportion to the ratio of masses, while any anomalous precession remains unaffected. The Extrasolar Planet Encyclopedia (<http://www.obspm.fr/encycl/encycl.html>) lists ten planets with  $e > 0.5$  currently known. These planets and their properties are described briefly in Table 2. They have masses typically of a Jupiter mass or more, and are (as yet) the only planets detected around their parent stars. Their orbital periods range from 62 d to 5.7 yr and thus observations of the systems could be expected to reveal any anomalous precession on a reasonable time-scale. For example, consider the extrasolar planet HD 3651b with  $e = 0.63$  and a period = 62.23 d (Fischer et al. 2003). If  $\delta = \pm 10^{-6}$ , then  $\theta \sim \pi \pm 2 \times 10^{-6}$ , giving an anomalous precession of  $10^{-4}$  deg per half-cycle. Given the orbital period of the planet, this would produce  $0^\circ 1$  of extra precession per century. Amounting to one part in a few thousand, this should be detectable with continued observations. Thus systems like this one, particularly if there is only one planet present or it is the most massive by far, can be expected to provide increasing refined constraints on  $\delta$ . Prospects for measuring the precession of high-eccentricity asteroids in our own Solar system where higher

**Table 2.** High-eccentricity extrasolar planets, listing their eccentricity and orbital period as well as their mass (in Jupiter masses) multiplied by the sine of the inclination of their orbit to the plane of the sky ( $M \sin I$ ).

	$M \sin I (M_{\text{Jup}})$	period (d)	$e$
HD 80606	3.41	$111.78 \pm 0.21$	$0.927 \pm 0.012$
$\iota$ Draconis	8.64	550.65	0.71
HD 222582	5.11	572.0	0.71
HD 89744	7.2	$256 \pm 0.7$	$0.7 \pm 0.02$
HD 2039	$4.85 \pm 1.7$	$1192 \pm 150$	$0.68 \pm 0.15$
16 Cygni B	1.69	798.9	0.67
HD 3651	0.2	62.23	0.63
HD 39091	10.35	2063.8	0.62
HD 147513	1.0	$540.4 \pm 4.4$	$0.52 \pm 0.08$
HD 1237	3.21	$133.82 \pm 0.2$	$0.505 \pm 0.018$

accuracies can be obtained are even better, though the effects of other perturbations complicates the analysis.

Given the recent increase in the number of high-eccentricity asteroids and improvements in radar detection techniques, as well as the discovery of massive high-eccentricity planets on short-period orbits around other stars, the ‘laboratory’ for the measurement of deviations from Newtonian gravity has expanded dramatically over the last decade. These advances provide the possibility of testing Newtonian gravity in new regimes of eccentricity, mass and other parameters, and the authors encourage observers in this regard.

### 3 THE CASE OF FORCE LAWS DIFFERING CONSIDERABLY FROM THE INVERSE SQUARE

We turn now to cases where  $\delta$  can be considerably larger, say 0.25 or 0.5. In such cases we may determine the apsidal angle by numerical integration. For our force law the potential energy is given by

$$V(r) = - \int_{\infty}^r (-r^{-N}) dr = \frac{r^{-N+1}}{-N+1},$$

where we have taken the gravitational constant and the central mass to be 1 and the case  $N = 1$  is excluded. The introduction of a cosmological constant  $\Lambda$  would result in

$$V(r) = \frac{r^{-N+1}}{-N+1} - \frac{\Lambda}{6} r^2$$

(Einstein 1917; Earman 2001). In addition, it is known that when  $N = 3$  the trajectory is a Cotes spiral, in which  $r$  goes to 0 or  $\infty$ . As our concern is with bounded orbits in the neighbourhood of  $N = 2$ , we shall mainly confine our investigation to the open interval [ $1 < N < 3$ ]. In this range  $V < 0$ . The total energy is

$$E = \frac{1}{2} \left[ \left( \frac{dr}{dt} \right)^2 + r^2 \left( \frac{d\theta}{dt} \right)^2 \right] + V(r). \quad (14)$$

The kinetic energy, given by the bracketed term on the right, is always positive, whence  $V < E$ . In order that the orbit be bounded away from  $r = 0$  and  $r = \infty$ , we must have  $E < 0$ .

For  $N = 1$ ,  $V(r)$  is the logarithmic potential characteristic of the singular isothermal sphere (Binney & Tremaine 1987). We give a brief analysis of the determination of  $\theta(e)$  for this case, by Touma & Tremaine (1997), separately at the end of this section.

We eliminate  $t$  from equation (14) by means of  $r^2(d\theta/dr) = h$ , the angular momentum. The result is simplified if we replace  $r$  by  $1/u$ . We thus obtain

$$\frac{du}{d\theta} = \frac{\sqrt{2}}{h} \left[ E + \frac{u^{N-1}}{N-1} - \frac{h^2 u^2}{2} \right]^{1/2}. \quad (15)$$

For  $du/d\theta$  to be real, the radicand on the right must be positive, and at each apse we must have  $du/d\theta = 0$ , the apsides being defined where the radicand on the right has real positive roots. Suppose the least root is  $u_1$  (for the higher apse) and the greatest is  $u_2$  (for the lower apse). Then the angle between higher and lower apsides, or ‘apsidal angle’, will be

$$\theta = \frac{h}{\sqrt{2}} \int_{u_1}^{u_2} \left[ E + \frac{u^{N-1}}{N-1} - \frac{h^2 u^2}{2} \right]^{-1/2} du. \quad (16)$$

The results in the inverse-square case have been shown earlier (Valluri et al. 1997) and  $\theta = \pi$ . This, of course, is an expected

**Table 3.** Apisidal angle and its derivative ( $N = 3/2$ ).

Eccentricity	Apisidal angle in degrees	$\partial\theta/\partial N$	$\theta - \theta_0$ (per cent deviation)
$e \ll 1$	146.969 ( $= \theta_0$ )	48.8	0
0.2	146.657	49.2	-0.312 (0.212 per cent)
0.4	145.641	50.4	-1.328 (0.904 per cent)
0.6	143.608	52.7	-3.361 (2.287 per cent)
0.8	139.530	57.7	-7.439 (5.062 per cent)
1.0	120.0	80.0	-27.00 (18.4 per cent)

result: the inverse-square law, when the orbit is bounded away from infinity, implies a fixed elliptical orbit with apsidal angle  $\pi$ .

In the case of a non-zero  $\Lambda$ , equation (15) becomes

$$\frac{du}{d\theta} = \frac{\sqrt{2}}{h} \left[ E + \frac{u^{N-1}}{N-1} - \frac{h^2 u^2}{2} - \frac{\Lambda}{6u^2} \right]^{1/2}. \quad (17)$$

This is expected to introduce a consequent additional perihelion shift for Mercury of  $\Lambda/5 \times 10^{-42} \text{ cm}^{-2} \text{ arcsec per century}$ , which is negligible as  $\Lambda \sim 10^{-58} \text{ cm}^{-2}$  (e.g. Rindler 1986). It is worth noting that the integration of equation (17) can be done in terms of elliptic functions (Goldstein 1990), and that the generalization of equation (15) leads to post-Newtonian orbits in the Schwarzschild space-time metric which give accurate values for the precession, for example, of Mercury or the binary pulsar system (Schutz 1996).

In equation (16), both  $E$  and  $h$  can be regarded as functions of the limits of integration,  $u_1$  and  $u_2$ . It follows that the apsidal angle  $\theta$ , for given  $N$ , is a function of  $u_1$  and  $u_2$  alone. Indeed, it is a function solely of the ratio  $u_1:u_2$ .

Using the MATHEMATICA program, we have integrated equation (16) by numerical integration for  $N = 3/2, 7/4, 9/4$  and  $5/2$ . As Whittaker (1961) observes, equation (16) can be solved in terms of elliptic functions when  $N = 3/2, 5/3, 7/3$  or  $5/2$ ; as elliptical functions are doubly periodic, the result of the integrations cannot be  $\pi$ . But we have chosen to apply a uniform program of numerical integration (Valluri et al. 1997). For each of our four values of  $N$ , we assigned  $E$  three different values ( $-2, -1, -0.5$ ), and for a series of values of  $h$  (400 in each case, with  $\Delta h = 0.001$ ), we computed the corresponding values of  $u_1$  and  $u_2$  from the radicand of equation (16). Finally, for each pair ( $u_1, u_2$ ), we carried out the numerical integration of equation (16) to obtain the apsidal angle  $\theta$ .

In Tables 3–6, for each of the four force laws investigated, we tabulate the apsidal angles  $\theta$  corresponding to eccentricities of 0.2, 0.4, 0.6, 0.8, as well as the apsidal angle  $\theta_0$  determined by Newton's or Bertrand's formula for very small eccentricity,  $\theta - \theta_0$ , and the percentage deviation of  $\theta$  from  $\theta_0$ . We will discuss the calculation of the derivative column in these tables shortly. A graph plotting apsidal angle against eccentricity, as determined by the numerical integrations in each case was determined (Valluri et al. 1997).

**Table 4.** Apisidal angle and its derivative ( $N = 7/4$ ).

Eccentricity	Apisidal angle in degrees	$\partial\theta/\partial N$	$\theta - \theta_0$ (per cent deviation)
$e \ll 1$	160.997	64.1	0
0.2	160.808	64.7	-0.189 (0.117 per cent)
0.4	160.194	66.7	-0.803 (0.499 per cent)
0.6	158.957	70.6	-2.040 (1.267 per cent)
0.8	156.438	78.5	-4.559 (2.832 per cent)
1.0	144.0	115.2	-17.00 (10.6 per cent)

**Table 5.** Apisidal angle and its derivative ( $N = 9/4$ ).

Eccentricity	Apisidal angle in degrees	$\partial\theta/\partial N$	$\theta - \theta_0$ (per cent deviation)
$e \ll 1$	207.846		0
0.2	208.132		+0.286 (0.138 per cent)
0.4	209.073	144.4	+1.227 (0.590 per cent)
0.6	210.981	153.0	+3.135 (1.508 per cent)
0.8	214.929	173.6	+7.083 (3.408 per cent)
1.0	239.5	320.0	+31.65 (15.23 per cent)

**Table 6.** Apisidal angle and its derivative ( $N = 5/2$ ).

Eccentricity	Apisidal angle in degrees	$\partial\theta/\partial N$	$\theta - \theta_0$ (per cent deviation)
$e \ll 1$	254.558		0
0.2	255.316		+0.758 (0.298 per cent)
0.4	257.795		+2.237 (1.272 per cent)
0.6	262.829	279.8	+8.271 (3.249 per cent)
0.8	273.275	315.1	+18.717 (7.353 per cent)
1.0	354.7	720.0	+100.1 (39.33 per cent)

In the particular case where  $e = 1$  (Valluri et al. 1997), the integral (16) can be reduced for  $N > 1$  to

$$\theta = \int_0^1 (u^{N-1} - u^2)^{-1/2} du. \quad (18)$$

which leads to the elliptic and hyperelliptic integrals. We observe that a logarithmic function for the potential results for  $N = 1$ . This, of course, is not the usual power law. Such a potential is unusual for motion about a point; it is rather more typical of a line source (Goldstein 1990). For  $N < 1$ , the potential is an increasing function of  $r$  and the apsidal angle is  $\pi/2$ . This is the same for the Hooke's law force. Numerical integration of this formula for our four values of  $N$ , namely  $3/2, 7/4, 9/4, 5/2$ , gives less accurate results than the analytical ones which were also shown for comparison (Valluri et al. 1997). The integral for  $e = 1$  (which is the limiting value of large  $e$  for bound orbits) can be exactly done in terms of the  $\Gamma$  (gamma) or  $\beta$  (beta) functions given below

$$\begin{aligned} \theta &= \frac{\Gamma\left(\frac{1}{2}\right) \Gamma\left[\frac{(1-N)/2+1}{3-N}\right]}{(3-N) \Gamma\left[1-\frac{1}{2}+\frac{(1-N)/2+1}{3-N}\right]} \\ &= \frac{\Gamma\left(\frac{1}{2}\right) \Gamma\left(\frac{1}{2}\right)}{(3-N) \Gamma(1)} = \frac{\pi}{3-N}. \end{aligned} \quad (19)$$

The derivative of  $\theta$  with respect to  $N$  then becomes

$$\frac{d\theta}{dN} = \frac{\pi}{(3-N)^2}. \quad (20)$$

The values corresponding to  $e = 1$  of  $d\theta/dN$  for  $N = 3/2, 7/4, 9/4$  and  $5/2$  are shown in Tables 3–6.  $\theta_0$  is the Newtonian value for the apsidal angle.  $\theta$  is the more exact value and the percent deviation from  $\theta_0$  is also indicated in the tables.

It can be observed from these results that precession increases for  $N > 2$ , and decreases for  $N < 2$ , with increasing eccentricity. The differences  $\theta - \theta_0$  are less than a degree for eccentricities less than 0.2, but rise nearly to  $100^\circ$  for  $e = 1$  when  $N = 5/2$ . Thus the curves  $\theta(e)$  turn away from the horizontal line  $\theta = \pi$  as  $e$  increases (Valluri et al. 1997).

We can use equation (16) to check the accuracy of this formula for very small  $\delta$ , although not, it seems, by a direct numerical integration: when  $|\delta|$  is very small, MATHEMATICA and MAPLE labour

for hours at the integration of equation (16), which turn out to be improper integrals, without producing a reliable result. Instead we have proceeded as follows. The derivative  $\partial\theta/\partial N$  obtained from formula (11) is  $90^\circ$  ( $\arcsin e/e$ ); this, multiplied by  $\delta$ , will give the amount of precession in a half-period. But we can obtain the derivative  $\partial\theta/\partial N$  also from equation (16) by differentiating under the integral sign. We first simplify equation (16) by expressing  $E$  and  $h$  in terms of the limits of integration, and (as the result depends only on the ratio  $u_2 : u_1$ ) stipulating that  $u_1 = 1$ . To achieve this, reverting to equation (15) and setting  $du/d\theta$  to 0 at  $u_1 = 1$  and  $u_2$  yields the two algebraic equations

$$E + \frac{1}{N-1} - \frac{h^2}{2} = 0 \quad (21)$$

and

$$E + \frac{u_2^{N-1}}{N-1} - \frac{h^2 u_2^2}{2} = 0. \quad (22)$$

Solving for  $E$  and  $h^2/2$  simultaneously from these two equations results in

$$E = \frac{u_2^{N-1} - u_2^2}{(N-1)(u_2^2 - 1)} \quad (23)$$

and

$$\frac{h^2}{2} = \frac{u_2^{N-1} - 1}{(N-1)(u_2^2 - 1)}, \quad (24)$$

where  $u_2$  is now the ratio of the greatest to the least distance from the centre, that is,  $r_M/r_m$ , so that

$$u_2 = \frac{1+e}{1-e}. \quad (25)$$

It is of interest to note that the case of imaginary eccentricity corresponds to orbits that plunge into the force centre and has two solutions (which are complex conjugates of each other) given by Hagihara (1931) and Chandrasekhar (1983). It is also worthwhile pointing out that the perihelion precession for Mercury in the Schwarzschild space-time has an analogous expression, the simplification being that one has to obtain the roots of a cubic equation (Schutz 1996). The solution in such a case would be given in terms of the Weierstrass elliptic functions (Boccaletti & Pucacco 1996).

With the above simplifications, the integral takes the form

$$\theta = (u_2^x - 1)^{1/2} \times \int_1^{u_2} [u_2^x(1-u^2) + (u_2^2-1)u^x + (u^2-u_2^2)]^{-1/2} du. \quad (26)$$

Clearly the apsidal angle depends only on  $N$  and  $u_2$  (or  $e$ ). The derivative of  $\theta$  with respect to  $x$  is shown below

$$\frac{\partial\theta}{\partial x} = \frac{u_2^x - 1}{2\sqrt{u_2^x - 1}} \times \int_1^{u_2} \frac{u_2^x(1-u^x) \ln u - u_2^x(1-u^x) \ln u_2}{[(1-u_2^x)u^2 - (1-u_2^2)u^x + u_2^x - u_2^2]^{3/2}} du, \quad (27)$$

where  $x = N - 1$ . This result is true for all  $x$  in the interval  $0 < x < 2$ . The integrand has discontinuities at both limits. The integral has a meaning by the limit process and has a finite value. Evaluating the

result at  $x = 1$  (so that  $N = 2$ ), we find

$$\frac{\partial\theta}{\partial x} = \frac{1}{2(u_2 - 1)} \times \left\{ \pi u_2 \ln u_2 - \int_1^{u_2} \frac{(1-u^2)u_2 \ln u_2 - (1-u_2^2)u \ln u}{[(u_2-u)(u-1)]^{3/2}} du \right\}. \quad (28)$$

The integrals on the right can be given in closed form in terms of generalized hypergeometric functions (GHGFs) and can also be expressed in terms of algebraic and logarithmic functions, which are given below, though much of the tedious algebra has been omitted.

$$\int_1^{u_2} \frac{(1-u^2)u_2 \ln u_2 - (1-u_2^2)u \ln u}{[(u_2-u)(u-1)]^{3/2}} du = \pi u_2 \ln u_2 - 2\pi(u_2+1) \left( \frac{\sqrt{u_2}-1}{\sqrt{u_2+1}} \right). \quad (29)$$

The expression from the GHGF reduces to that given in equation (29). Thus, for the special case of  $N = 2$ , the exact solutions are  $\theta = \pi$  and

$$\begin{aligned} \frac{\partial\theta}{\partial N} &= \pi \left( \frac{u_2+1}{u_2-1} \right) \left( \frac{\sqrt{u_2}-1}{\sqrt{u_2+1}} \right) \\ &= \frac{\pi}{1+\sqrt{1-e^2}} = \frac{\pi(1-\sqrt{1-e^2})}{e^2} \\ &\sim \frac{\pi}{2} \left( 1 + \frac{e^2}{4} + \frac{e^4}{8} + \dots \right) \end{aligned} \quad (30)$$

which is identical to the approximation (for small  $e$ ) given by equation (12). This exact solution for  $\partial\theta/\partial N$  ( $N = 2$ ) clearly shows that the approximate method for obtaining the apsidal angle  $\theta$  given in the paper of (Valluri et al. 1997) really uses the first derivative term of the Taylor expansion of  $\theta(e, N)$  in obtaining approximate values for  $\theta$  in the region around  $N = 2$ . Equation (12) is understandably not an approximation in the usual sense and is much more accurate than equation (11).

We have checked by numerical integration, and have thus evaluated equation (28) for the values of  $u_2$  that correspond to eccentricities of 0.2, 0.4, 0.6, 0.8, namely  $3/2, 7/3, 4$  and  $9$ . The results of our comparison, in degrees per unit  $N$ , are shown in Table 7.

We can also compute  $\partial\theta/\partial h$ , where  $h(e, N)$  is the angular momentum of the orbit. Though  $h$  is constant in the Kepler case, in systems where dissipation is important this constraint vanishes, and the induced precession can be modelled by a consideration of  $\partial\theta/\partial h$ .

By the chain rule

$$\frac{\partial\theta}{\partial N} = \frac{\partial\theta}{\partial h} \frac{\partial h}{\partial N} \quad (31)$$

where we have used  $\theta = \theta(N, e)$  or  $\theta = \theta(N, h)$ . Therefore

$$\frac{\partial\theta}{\partial h} = \frac{\partial\theta}{\partial N} \left( \frac{\partial h}{\partial N} \right)^{-1}. \quad (32)$$

**Table 7.** Derivatives of  $(\partial\theta/\partial N)$  ( $N = 2$ ) for different eccentricity  $e$ .

$e$	(29)	(12)	Quartic	Cubic	Finite difference
0.2	90.92	90.92	89.98	89.97	89.98
0.4	93.92	93.89	92.96	92.94	92.96
0.6	100.00	99.56	98.97	98.98	98.99
0.8	112.50	109.01	111.50	111.40	111.39

From equation (24) we can compute

$$\frac{\partial h}{\partial N} = \frac{1}{h} \left( \frac{u_2^{N-1}(N-1) \ln u_2 - u_2^{N-1} + 1}{(N-1)^2(u_2^2 - 1)} \right). \quad (33)$$

Combining equation (33) with equation (30) we obtain

$$\frac{\partial \theta}{\partial h} = \frac{\pi h(u_2 + 1)(\sqrt{u_2} - 1)((N-1)^2(u_2^2 - 1))}{(u_2 - 1)(\sqrt{u_2} + 1)(u_2^{N-1}(N-1) \ln u_2 - u_2^{N-1} + 1)}. \quad (34)$$

This equation will be singular where the denominator is zero. This criteria in particle-scattering theory determines the location of scattering resonances. Given the importance of resonances to the gravitational  $N$ -body problem, we examine this situation further.

Assuming  $e < 1$  and taking the case  $N = 2$ , the denominator of equation (34) is zero where

$$u_2 \ln u_2 - u_2 + 1 = 0. \quad (35)$$

From a mathematical view point, it is interesting that this equation is related to the Lambert  $W$  function  $f(W) = W \exp(W)$  (Corless et al. 1996). Rewriting equation (35) we find

$$\frac{1}{u_2} = -W_0[-\exp(-1)], \quad (36)$$

where  $W_0$  is the principal branch of the multivalued Lambert  $W_k$  function with branch index  $k = 0$ . Recalling that  $u_2 = (1 + e)/(1 - e)$ , the solution to this equation is  $u_2 \approx -3.5911214$  or  $e \approx 1.77$ . This is in conflict our earlier assumption of an elliptic orbit, and indicates this condition is not satisfied on the principal branch for  $N = 2$ . The trivial solution  $u_2 = 1$  gives  $e = 0$  for which the apsidal line is not defined.

We also present the values of the derivatives obtained by application of Lagrangian interpolation and finite difference methods to the data points of Tables 3–6. The use of all five data points gives a quartic equation whereas we obtain two cubic equations by use of the first four and last four data points. The slope of the curve at  $N = 2$  is obtained from a single differentiation of the quartic; the slopes for the cubic at  $N = 2$  are averaged. The results from both of these methods agree very nearly (Wilson, private communication). The values in Table 7 are in good agreement with each other; the discrepancies from the correct values are less than or about 1 per cent of the correct values. This deviation is possibly owing to the scarcity of data points. We conclude that the curves  $\theta(e)$  are smooth. Another way to show this is to use the first derivative given in equation (30), which indicates that the first-order approximation of  $\theta(e)$  in the vicinity of  $N = 2$  is a smooth function for all  $e$ . Equation (30) can be used to determine  $\theta$  in the neighbourhood of  $N = 2$  for all  $e$ . The derivative of the complete solution of the Mathieu–Hill differential equation with respect to  $\delta (= N - 2)$  gives a smooth and finite value (Valluri et al. 1999).

We observe that Newton’s formula implies that  $\partial\theta/\partial N$  is always  $90^\circ$  for  $x = 1$  ( $N = 2$ ) irrespective of the eccentricity  $e$ . The integration of equation (28) shows that, for an eccentricity of 0.2, our factor  $\arcsin e/e$  gives an apsidal precession that is 0.34 per cent shy of the correct value. With this correction, Asaph Hall’s value of  $\delta$  gives 43.35 arcsec of precession per Julian century, differing from the empirical value he assumed (43 arcmin) by less than the observational uncertainty.

It is instructive to present plots of  $\theta$ ,  $\partial\theta/\partial N$ ,  $E$  and  $h$  versus  $e$  or  $1/u_2$  ( $=r_m/r_M$ ) for select values of  $N$ .  $e$  and  $N$  act as independent variables for  $\theta$ ,  $\partial\theta/\partial N$ ,  $E$  and  $h$ , which depend only on  $N$  and  $e$ .

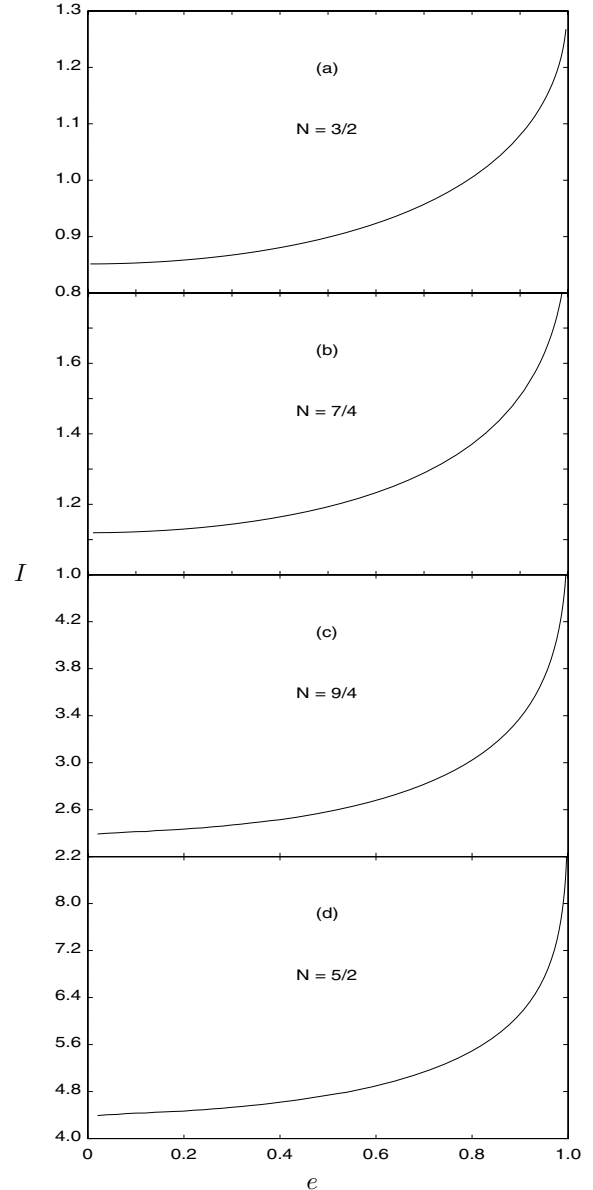


**Figure 1.** The function  $I(e)$  for different values of  $N$ : (a)  $N = 3/2$ , (b)  $N = 7/4$ , (c)  $N = 9/4$ , (d)  $N = 5/2$ .

Parts (a)–(d) of Figs 1–6 study the variation for

- (1)  $\partial\theta/\partial N$  ( $=I$ ) as a function of  $e$  for different  $N$ ,
- (2)  $\theta$  as a function of  $e$  for different  $N$ ,
- (3)  $E$  as a function of  $e$  for different  $N$ ,
- (4)  $E$  as a function of  $N$  for different  $e$ ,
- (5)  $h$  as a function of  $e$  for different  $N$ ,
- (6)  $h$  as a function of  $N$  for different  $e$ .

The values of  $I$  increase for higher  $N$ . Figs 7 and 8 show the three-dimensional graphs for  $E(e, N)$  and  $h(e, N)$ . Figs 9 and 10 show the three-dimensional graphs for  $\theta(e, N)$  and  $\partial\theta/\partial N(e, N)$ .

We have also asked the following interesting question: is it possible that, with the eccentricity increasing in a continuous fashion, the apsidal precession might diminish continuously and finally, at some value of the eccentricity, become zero? We could not find any evidence for such isolated cases of apsidal quiescence.

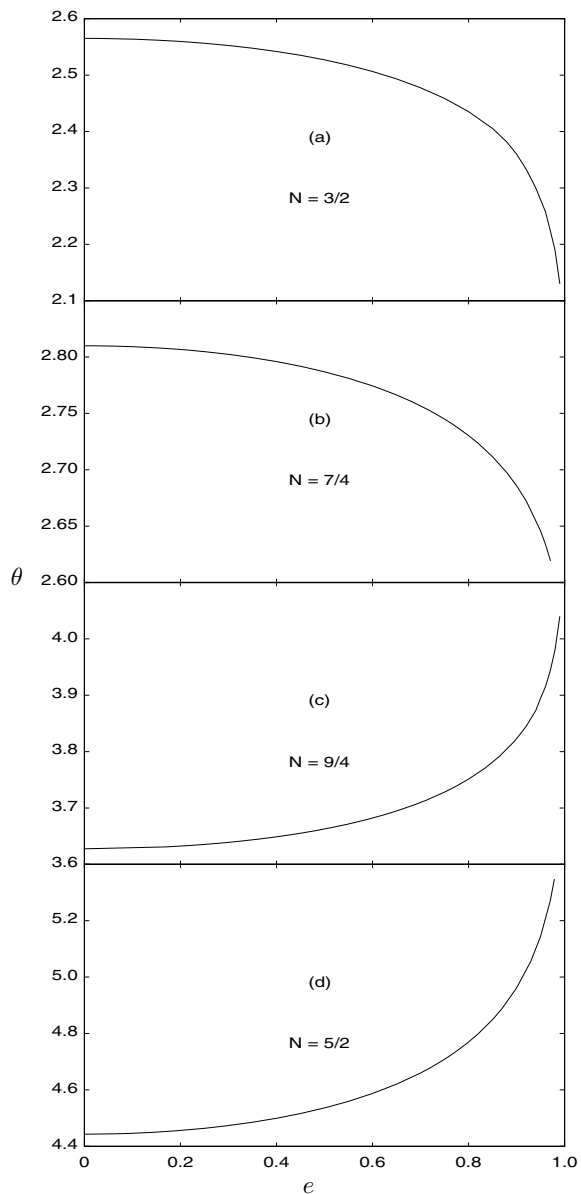


**Figure 2.** The function  $\theta(e)$  for different values of  $N$ : (a)  $N = 3/2$ , (b)  $N = 7/4$ , (c)  $N = 9/4$ , (d)  $N = 5/2$ .

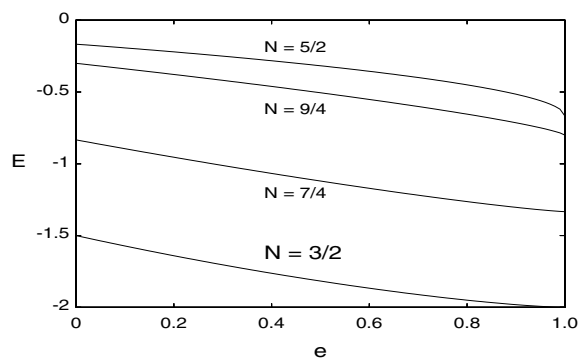


**Figure 3.**  $E$  versus  $e$ .

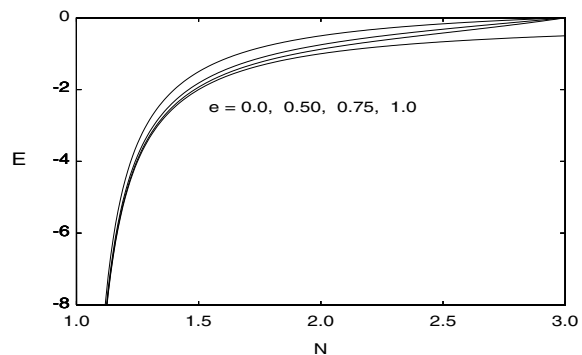


**Figure 4.**  $E$  versus  $N$ .

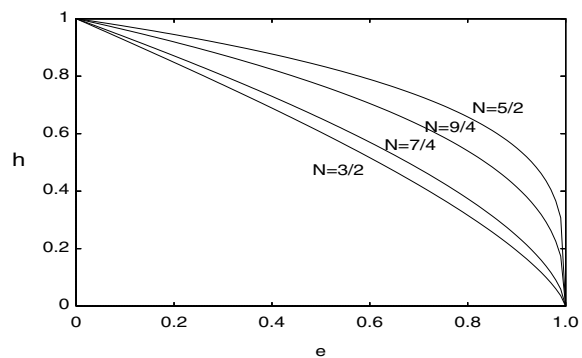


**Figure 5.**  $h$  versus  $e$ .

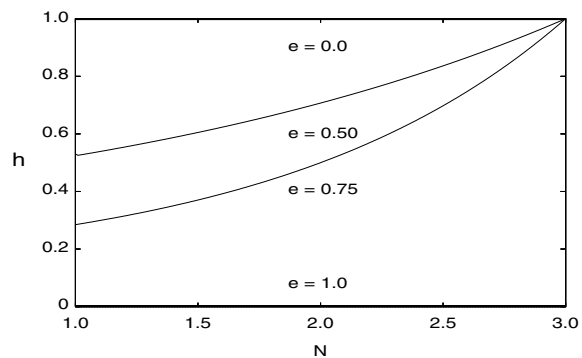


**Figure 6.**  $h$  versus  $N$ .

The Logarithmic Potential ( $N = 1$ ): The logarithmic potential is a planar non-axisymmetric power-law potential. Touma & Tremaine (1997) have studied the dynamics of eccentric orbits for such a potential as well as their power law obtained by a symplectic mapping. They study the orbit structure of non-axisymmetric potentials relevant to galaxies. In the case of a scale-free spherical potential the expression for the precession rate (in their notation)

$$g(\alpha, y) = 2h(\alpha)y \int [2 \ln u - u^2 y^2 h^2(0)]^{1/2} du, \quad (37)$$

where  $\alpha = 0$  is the logarithmic potential,  $h(0) = e^{-1/2}$ ,  $y = L/L_c(E)$  for  $-1 \leq y \leq 1$ .  $E = 1/2 + \ln r_c$  ( $\alpha = 0$  is the dimensionless angular momentum (for a circular orbit with radius  $r_c$ ). Here,  $L_c(E) = e^{-1/2} e^E \equiv h(0) e^E$  and  $g(\alpha, y) = 2\pi P_r/P_\phi$  where  $P_r$  and  $P_\phi$  are

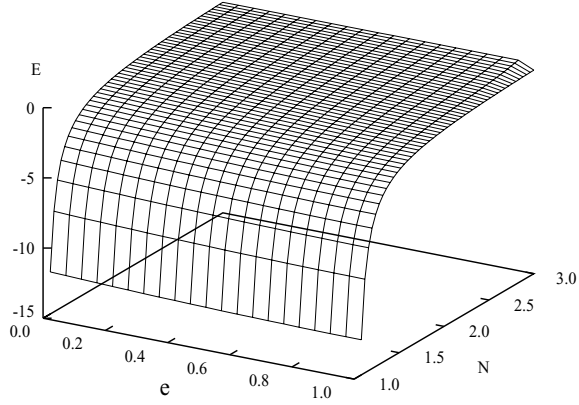


**Figure 7.** Three-dimensional graph for function  $E(e, N)$ .

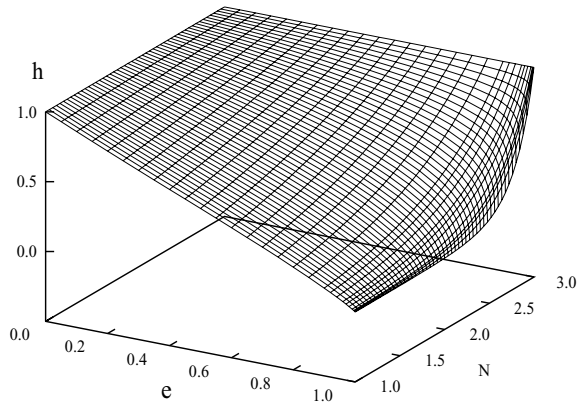


**Figure 8.** Three-dimensional graph for function  $h(e, N)$ .

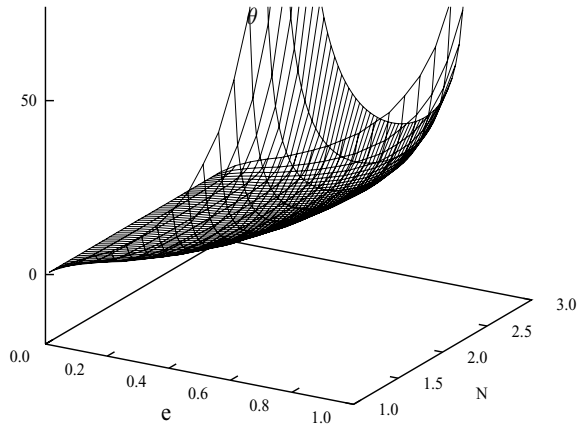


**Figure 9.** Three-dimensional graph for function  $\theta(e, N)$ .

the radial and azimuthal periods. For near radial orbits, they find  $\lim_{y \rightarrow 0_{\pm}} g(\alpha, y) \equiv \pm g_0(\alpha) = \pm \pi \quad (\alpha \geq 0)$ .

In general, the precession rate is a function of the energy of the orbit. The symplectic map remains unchanged. The value will be halved for half of the complete orbit.

We were able to obtain this value by first finding the roots of the denominator of the integrand by the use of the function (Lambert  $W$  function), one that has seen a renaissance among physicists and mathematicians in recent years (e.g. Cranmer 2004; Warburton &

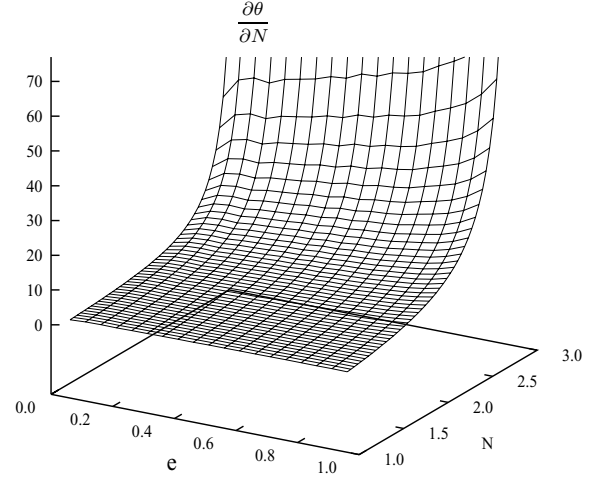


**Figure 10.** Three-dimensional graph for function  $\frac{\partial \theta}{\partial N}(e, N)$ .

**Table 8.** Numerical integration results for  $g_0(\alpha)$ .

	$h(0)$	$y(0)$	$E$	Integral
1	$e^{-\frac{1}{2}}$	$3.314201e-2$	$-e^{-1}$	$3.14168841052944936010$
2	$e^{-\frac{1}{2}}$	$12.257e-3$	$-e^{-0.844}$	$3.14164760003483989337$
3	$e^{-\frac{1}{2}}$	$20.01375e-4$	$-e^{-0.84303}$	$3.14149690810185111545$

Wang 2004). The definition of  $W$  is that it is the multivalued function that solves the equation (Corless et al. 1996)

$$W e^W = Z \quad (38)$$

where  $Z$  is complex.

The integral

$$\int_{0.37}^5 \frac{2 y(0) h(0)}{\sqrt{(2x + 2E)e^{-2x} - y^2(0) h^2(0)}} dx \quad (39)$$

was evaluated using a ten-point Gaussian quadrature C program. The limits of integration are the roots of the radical in the integrand. These were obtained from a MAPLE plot. The results are summarized in Table 8. As expected, the integral evaluates to  $\pi$ . Also note that varying  $h(0)$  will result in a wider range of  $y(0)$  values. It should be pointed out the roots of the denominator of the integrand,  $(2x + 2E)e^{-2x} - y^2(0) h^2(0)$ , determines the limits of the integration.

Touma & Tremaine (1997) provide an asymptotic power series for  $g(\alpha, y)$  by use of the Mellin transformation followed by the inverse Mellin transformation.

Newton had found, in orbits differing from circles, very special force laws giving rise to orbit closure. He assumed it quite unlikely that such closure could arise under other laws for isolated values of the eccentricity  $e$  – clearly a radical departure from the systematic order he helped discover. He rightly inferred in Proposition I.45 that the relation between force law and orbit shape was one of mutual implication. Modern classical mechanics proves that zero precession implies the inverse-square force law by means of the Runge–Lenz or eccentricity vector – a vector which points from the origin to the pericentre, and is a constant of motion if and only if the force is inverse square (Chandrasekhar 1995; Goldstein 1975). The Runge–Lenz vector of length  $e$  in the orbital plane ensures the fixity in space (or in Newton’s terminology ‘the quiescence of the aphelion points’) of the direction of the major axis of the elliptic orbits.

Newton's assurance was more, perhaps from a general view of the relation between the orbital species and central force types. From Proposition 9 and 41 of Book I he proved that for the  $1/r^3$  force law, the path of the body will be an equiangular spiral, spiralling into the centre or out to infinity unless the initial conditions are just right for circular motion. Thus for the force law  $1/r^3$ , there can be no apsides. Here the force law determines the character of the curve, and conversely.

In his correspondence with Hooke during 1679–80 (see Turnbull 1960; Nauenberg 1994), Newton argues that in a uniform central force field [ $f(r) = \text{constant}$ ], a projected body would move in a trajectory something like a trefoil but not reentrant. The angle then between upper and lower apse would be between  $90^\circ$  and  $180^\circ$ . It seems likely that he constructed this orbit in discrete steps using the fact that the curvature goes directly as the force and inversely as the square of the velocity, and in addition using the reflective property for any orbit in a central force field (Nauenberg 1994): the trajectory from apo to pericentre is obtained as a mirror image of the trajectory from peri to apocentre, combined with a rotation. Constructing the orbits in discrete steps is a process that is unavoidably inaccurate. Proposition 45 proves his generalization for the apsidal angle for cases in which eccentricity is negligible. Only in two cases would the orbit be fixed and reentrant: when  $N = 2$ , and when  $N = -1$ . In the second edition of the Principia, Newton showed these two reentrant orbits to be dual to one another in the following sense: the law of force for the one can be derived from that for the other by an appropriate shift in the centre of force (from focus to the centre of the ellipse or vice versa). Both these orbits are related by a quadratic mapping in the complex plane. Moreover, Newton's work has given an amazingly modern proof from a topological perspective of the transcendence of Abelian integrals as it was based on the topology of Riemann surfaces (Arnold & Vasil'ev 1989). We believe that Newton's precession theorem is also of interest from the perspective of the invertibility of Abelian integrals relative to algebraic curves, the genus of the corresponding algebraic equations and the Lambert  $W$  function. Riemann's methods based on the topology of Riemann surfaces will be relevant in such a study (Nobile 1908).

#### 4 CONCLUSIONS

We have shown that the apsidal angle  $\theta(N, e)$  for each  $N$  in the interval  $(1, 3)$  is a smooth and continuous function of  $e$ . We have also applied the analytical results to the calculations of the lunar orbit and Mercury's perihelion. In addition, we found that  $\partial\theta/\partial e$ ,  $\partial^2\theta/\partial e^2$ ,  $\partial\theta/\partial N$  and  $\partial^2\theta/\partial N^2$  are all continuous, i.e. there is no evidence for isolated cases of apsidal quiescence. The apsidal angle and its derivative are also calculated for the special case  $e = 1$  in the interval  $1 < N < 3$ .

From a physical point of view, the slow lunar precession of  $1^\circ 5$  per half revolution owing to the action of the Sun perturbing the Earth–Moon system or the precession of the perihelion of Mercury does indicate that the precession theorem can be used to measure inverse-square variation even if precession owing to perturbation is present. For any body in orbit for which perturbation accounts for all of the precession, the zero unaccounted for precession counts as a null experiment measuring inverse-square variation. Increase of the eccentricity increases the amount of precession that results owing to a deviation from the inverse square. This suggests a null experiment with the absence of unexplained orbital precession a more appropriate measure of inverse-square variation of a centripetal force. Exciting possibilities are offered by recent discoveries of asteroids

and extrasolar planets. These bodies provide new opportunities for new high-precision tests of the form of the gravitational force law.

The introduction of mean gravitational field potentials generated by many bodies to study the motion of a single body under the reasonable assumption that it does not appreciably disturb the external field is a useful technique particularly in the study of the difficult  $N$ -body problem. Such an approach offers interesting aspects of a variety of applications in galactic dynamics and other fields. In such a context, spherically, axially and spheroidally symmetric potentials are of relevance (Boccaletti & Pucacco 1996) and mathematically tractable. Some of the mathematical analysis in this paper might be useful in such a study.

In addition, recent findings of satellites of asteroids raise interesting questions on the formation and the gravitational non-spherical potentials or force laws that describe their interaction. Touma & Tremaine (1997) have shown that potentials relevant in the morphology of orbits in triaxial potentials determine the structure of triaxial galaxies. Power-law potentials generated by power-law densities have singular behaviour and they indicate that such potentials could also be caused by massive BHs at the centres of many nearby galaxies. The high-resolution *Hubble Space Telescope* (*HST*) photometry of nearby elliptical galaxies and spiral bulges has provided support for the relevance of power-law potentials. Such studies as well as those on gravitational wave sources associated with the orbital decay of binary BH pairs that raise interesting questions on the coordinate dependence of semimajor axis and eccentricity (Damour & Deruelle 1985; Junker & Schaefer 1992) may further elucidate features of orbital dynamics.

#### ACKNOWLEDGMENTS

Valluri, Yu and Wiegert acknowledge financial support for this work from the Natural Sciences and Engineering Research Council of Canada (NSERC). The authors thank Mr John Drozd who performed the numerical integration of the last equation and prepared Table 8. We also thank Professor Scott Tremaine (Princeton), Professor S. Basu (The University of Western Ontario), Professor Curtis Wilson (St. John's College, Annapolis) and the anonymous referee for their constructive suggestions regarding the paper.

#### REFERENCES

- Arnold V. I., Vasil'ev V. A., 1989, Notices Am. Math. Soc., 36, 1148
- Barack L., Cutler C., 2004, Phys. Rev. D, 69, 2005
- Bertrand J., 1873, Comp. Rendus Séances Acad. Sci., Séance du lundi, T.XXVII, 849
- Binney J. J., Tremaine S., 1987, Galactic Dynamics. Princeton Univ. Press Princeton
- Boccaletti D., Pucacco G., 1996, Theory of Orbits Vol. I. Springer-Verlag, New York
- Brown E. W., 1895, An Introductory Treatise on the Lunar Theory. Cambridge Univ. Press (Republished 1960 by Dover Publications Inc., New York)
- Brown E. W., 1903, MNRAS, 64, 396
- Chandrasekhar S., 1983, The Mathematical Theory of Black Holes. Clarendon Press, Oxford
- Chandrasekhar S., 1995, Newton's Principia for the Common Reader. Clarendon Press, Oxford
- Chesley S. R. et al., 2003, Sci, 302, 1739
- Clemence G. M., 1947, Rev. Modern Phys., 19, 361
- Corless R. M., Gonnet G. H., Hare D. E. G., Jeffrey D. J., Knuth D. E., 1996, Adv. Comp. Math., 5, 329
- Cranmer S. R., 2004, Am. J. Phys., 72, 1397
- Damour T., Deruelle N., 1985, Ann. Inst. H. Poincaré, 43, 107

- Earman J., 2001, *Arch. Hist. Exact Sci.* 55, 189
- Earman J., Janssen M., 1993, in Earman J., Janssen M., Norton J. D., eds, *Einstein's Explanation of the Motion of Mercury's Perihelion*. Birkhäuser, Boston, p. 5
- Einstein A., 1915, *Erklärung der Perihelbewegung des Merkur aus der allgemeinen Relativitätstheorie*. Königlich Preussische Akademie der Wissenschaften, Sitzungsberichte, Berlin
- Einstein A., 1917, *Kosmologische Betrachtungen zur allgemeinen Relativitätstheorie*, Königlich Preussische Akademie der Wissenschaften, Berlin, Sitzungsberichte, pp. 142–152
- Festou M. C., 1986, in Lagerkvist C. I., Lindblad B. A., Lundstedt H., Rickman H., eds, *Asteroids, Comets and Meteors*. Vol II, Uppsala Univ. Press, Uppsala, p. 299
- Festou M. C., Rickman H., West R. M., 1993, *Ann. Rev. Astron. Astrophys.*, 4, 363
- Fischer D. A., Butler R. P., Marcy G. W., Vogt S. S., Henry G. W., 2003, *Astrophys. J.*, 590, 1081
- Glampedakis K., Andersson N., 2001, *Classical and Quantum Gravity*, 18, 1939
- Goldstein H., 1975, *Am. J. Phys.*, 43, 737
- Goldstein H., 1990, *Classical Mechanics*, 3rd edn. Addison Wesley, Reading, MA
- Hagihara Y., 1931, *Japan. J. Astron. Astrophys.*, 8, 67
- Hall A., 1894, *Astron. J.*, 14, 49
- Junker W., Schaefer G., 1992, *MNRAS*, 254, 146
- Le Verrier U. J. J., 1859, *Annales de l'Observatoire Impériale de Paris*, V, 1
- Levison H. F., Morbidelli A., Dones L., Jedicke R., Wiegert P. A., Bottke W. F., 2002, *Sci*, 296, 2212
- McLachlan N. W., 1947, *Theory and Application of Mathieu Functions*. Clarendon Press, Oxford, p. 133
- Nauenberg M., 1994, *Arch. Hist. Exact Sci.*, 46, 221
- Newcomb N. S., 1882, *Astron. Papers Prepared Use Am. Ephemeris Nautical Almanac*, I, 472
- Newton I., 1687, *Mathematical Principles of Natural Philosophy*. English translation: I. B. Cohen and A. Whitman. University of California Press, Los Angeles, 1998
- Nobile V., 1908, *Giornale di Matematiche di Bataglini*, 46, 313
- Peters P. C., 1964, *Phys. Rev.*, 136, B1224
- Peters P. C., Mathews J., 1963, *Phys. Rev.*, 131, 435
- Pierro V., Pinto I. M., Spallicci di F., A. D. A. M., 2002, *MNRAS*, 334, 855
- Regge T., Wheeler J. A., 1957, *Phys. Rev.*, 108, 1063
- Rickman H., 1986, in Melita O., ed., *ESA SP-249, The Comet Nucleus Sample Return Workshop*. ESA Publications Division, Noordwijk, p. 195
- Rindler W., 1986, *Essential Relativity*. Springer-Verlag, Berlin
- Romo W. J., Valluri S. R., 1998, *Nucl. Phys. A*, 636, 467
- Roseveare N. T., 1982, *Mercury's Perihelion from Le Verrier to Einstein*. Clarendon Press, Oxford
- Schutz B. F., 1996, *A First Course in General Relativity*. Cambridge Univ. Press, Cambridge
- Sekanina Z., 1964, *Bull. Astron. Inst. Czech.*, 15, 8
- Touma J., Tremaine S., 1997, *MNRAS*, 292, 905
- Turnbull H. W., ed., 1960, *The Correspondence of Isaac Newton*. Cambridge Univ. Press, Cambridge, p. 308
- Valluri S. R., Wilson C., Harper W. L., 1997, *J. Hist. Astron.*, 28, 13
- Valluri S. R., Romo W. J., 1989, *Nucl. Phys. A*, 492, 493
- Valluri S. R., Romo W. J., 1994, *Nucl. Inst. Meth. Phys. Res.*, B90, 589
- Valluri S. R., Biggs R. G., Harper W. L., Wilson C., 1999, *Can. J. Phys.*, 77, 393
- Valluri S. R., Jeffrey D. J., Corless R. M., 2000, *Can. J. Phys.*, 78, 823
- Warburton R. D. H., Wang J., 2004, *Am. J. Phys.*, 72, 1404
- Whittaker E. T., 1961, *A Treatise on the Analytical Dynamics of Particles and Rigid Bodies*, 4th edn. Cambridge Univ. Press, Cambridge
- Wilhelm K., 1987, *Nat*, 327, 27

This paper has been typeset from a  $\text{\TeX}/\text{\LaTeX}$  file prepared by the author.